

APPARENT THERMAL EMITTANCE OF CYLINDRICAL ENCLOSURES WITH AND WITHOUT DIAPHRAGMS*

GAETANO ALFANO

Istituto di Fisica Tecnica della Facoltà di Ingegneria di Napoli, Italy

(Received 26 January 1972 and in revised form 18 May 1972)

NOMENCLATURE

A ,	surface area;
A_o ,	overall enclosure surface;
L ,	cavity length;
L' ,	dimensionless cavity length, $=L/R$;
R ,	cavity radius;
R_i ,	diaphragm opening radius;
R'_i ,	dimensionless diaphragm opening radius, $=R_i/R$;
r ,	radial coordinate;
r' ,	dimensionless radial coordinate, $=r/R$;
T ,	absolute temperature;
x ,	axial coordinate;
x' ,	dimensionless axial coordinate, $=x/R$;
x'_0 ,	typical value of x' ;
δ ,	positive number;
ε ,	thermal emittance;
ε_a ,	apparent thermal emittance;
σ ,	Stefan-Boltzmann constant.

Subscripts

- 1, refers to diaphragm;
- 2, refers to bottom.

Superscripts

- 0, refers to starting functions in the iterative method;
- n , refers to the n th iteration.

INTRODUCTION

THE KNOWLEDGE of cavities apparent thermal emittance is of great practical interest in pirometry and in thermal radiation characteristics measurements where cavities are used as blackbody.

This note deals with isothermal cylindrical enclosures with and without circular diaphragms (Fig. 1). We used the "radiosity method" by which Sparrow [1] and Peavy [2] evaluated apparent emittance of cylindrical enclosures without diaphragms. Thus, four hypotheses underlie the achieved results: (1) isothermal surfaces, (2) diffuse reflected energy, (3) diffuse emitted energy, (4) gray surfaces. However if

surfaces are not gray, achieved results represent monochromatic apparent thermal emittance.

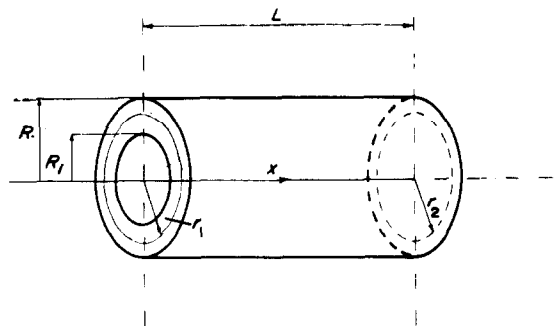


FIG. 1. Schematic diagram of cylindrical enclosure with diaphragm.

Cylindrical enclosures with circular diaphragms were previously analyzed by Gouffé [3] and by Quinn [4] but their methods are more approximated and besides they determined only the bottom apparent thermal emittance.

ANALYSIS

For a cylindrical enclosure closed by circular diaphragms at a typical position on the diaphragm, on the bottom and on the cylindrical surface a radiant flux balance can be written in dimensionless form respectively:

$$\varepsilon_a(r'_1) = \varepsilon + (1 - \varepsilon) \int_0^{L'} \varepsilon_a(x') dF_{dA(r'_1) - dA(x')} + (1 - \varepsilon) \int_0^{L'} \varepsilon_a(r'_2) dF_{dA(r'_1) - dA(r'_2)} \quad (1)$$

$$\varepsilon_a(r'_2) = \varepsilon + (1 - \varepsilon) \int_0^{L'} \varepsilon_a(x') dF_{dA(r'_2) - dA(x')} + (1 - \varepsilon) \int_{R'_i}^1 \varepsilon_a(r'_1) dF_{dA(r'_2) - dA(r'_1)} \quad (2)$$

$$\varepsilon_a(x'_0) = \varepsilon + (1 - \varepsilon) \int_0^{L'} \varepsilon_a(r'_2) dF_{dA(x'_0) - dA(r'_2)} + (1 - \varepsilon) \int_0^{L'} \varepsilon_a(x') dF_{dA(x'_0) - dA(x')} + (1 - \varepsilon) \int_{R'_i}^1 \varepsilon_a(r'_1) dF_{dA(x'_0) - dA(r'_1)} \quad (3)$$

* This work was supported by the Consiglio Nazionale delle Ricerche.

with $([1, 5, 6])$:

$$\begin{aligned} dF_{dA(r'_1) - dA(x')} &= \frac{2x'(x'^2 + 1 - r'_1{}^2)}{[(x'^2 + r'_2{}^2 + 1)^2 - 4r'_1{}^2]^{3/2}} dx' \\ dF_{dA(r'_1) - dA(r'_2)} &= \frac{2r'_2 L'^2 (r'_1{}^2 + r'_2{}^2 + L'^2)}{[(r'_1{}^2 + r'_2{}^2 + L'^2)^2 - 4r'_1{}^2 r'_2{}^2]^{3/2}} dr'_2 \\ dF_{dA(r'_2) - dA(x')} &= \frac{2(L' - x')[(L' - x')^2 + 1 - r'_2{}^2]}{\{[(L' - x')^2 + r'_2{}^2 + 1]^2 - 4r'_2{}^2\}^{3/2}} dx' \\ dF_{dA(r'_2) - dA(r'_1)} &= \frac{2r'_1 L'^2 (r'_1{}^2 + r'_2{}^2 + L'^2)}{[(r'_1{}^2 + r'_2{}^2 + L'^2)^2 - 4r'_1{}^2 r'_2{}^2]^{3/2}} dr'_1 \\ dF_{dA(x'_0) - dA(r'_2)} &= \frac{2(L' - x'_0)r'_2[(L' - x'_0)^2 + 1 - r'_2{}^2]}{\{[(L' - x'_0)^2 + r'_2{}^2 + 1]^2 - 4r'_2{}^2\}^{3/2}} dr'_2 \\ dF_{dA(x'_0) - dA(x')} &= \frac{1}{2} \left\{ 1 - |x'_0 - x'| \frac{(x' - x'_0)^2 + 6}{[(x' - x'_0)^2 + 4]^{3/2}} \right\} dx' \\ dF_{dA(x'_0) - dA(r'_1)} &= \frac{2r'_1 x'_0 (x'_0{}^2 + 1 - r'_1{}^2)}{[(x'_0{}^2 + r'_1{}^2 + 1)^2 - 4r'_1{}^2]^{3/2}} dr'_1. \end{aligned}$$

Equations (1)–(3) constitute a system of integral equations.

For an enclosure without diaphragm the equation (1), the last term of the equation (2) and the last term of the equation (3) disappear and so we find again the well known system of two integral equations [1, 2].

PROCEDURE

For these integral equations systems a closed-form solution is not possible. We used the method of successive approximations [7], already used by Sparrow [1] and by Peavy [2]. For cylindrical enclosures with diaphragms first we fix the enclosure characteristics: L' , R'_i and ϵ . Next we choose two arbitrary functions for $\epsilon_a(x')$ and $\epsilon_a(r'_2)$, we say $\epsilon_a^0(x')$ and $\epsilon_a^0(r'_2)$, and by equation (1) we obtain a first trial solution for $\epsilon_a(r'_1)$, we say $\epsilon_a^1(r'_1)$. From $\epsilon_a^1(r'_1)$ and $\epsilon_a^0(x')$ by equation (2) we obtain a first trial solution for $\epsilon_a(r'_2)$, $\epsilon_a^1(r'_2)$, and from $\epsilon_a^1(r'_1)$, $\epsilon_a^1(r'_2)$ and $\epsilon_a^0(x')$ by equation (3) we obtain a first trial solution for $\epsilon_a(x')$, $\epsilon_a^1(x')$. Iterating these operations from the first trial solutions $\epsilon_a^1(r'_1) - \epsilon_a^1(r'_2)$ and $\epsilon_a^1(x')$ we obtain the second trial solutions, $\epsilon_a^2(r'_1) - \epsilon_a^2(r'_2)$ and $\epsilon_a^2(x')$. Generally after n iterations we obtain $\epsilon_a^n(r'_1) - \epsilon_a^n(r'_2)$ and $\epsilon_a^n(x')$.

The procedure stops when we find

$$|\epsilon_a^n - \epsilon_a^{n-1}| < \delta \quad (4)$$

for any value of r'_1 in the range $R'_i - 1$, of r'_2 in the range 0–1 and of x' in the range 0– L' . In the (4) δ is a previously fixed positive value depending upon the desired approximation.

Using the successive approximations method, equations (1)–(3) become sums of integrals. Their solution was obtained numerically by Simpson's one third rule. Calculations were performed by the CDC G 20 electronic digital computer of Engineering Faculty of Naples.

RESULTS

We obtain results for $L' = 2-4$ and 8, for $\epsilon = 0.25-0.50$ and 0.75 and for $R'_i = 0.40-0.60$ and 0.80. To compare our calculation techniques with Sparrow's and Peavy's, we carried out solutions also for $R'_i = 1$, that is for enclosures without diaphragm. In the numerical integration we used as step sizes $\Delta x' = 0.04$ and $\Delta r'_1 = \Delta r'_2 = 0.025$; for δ we used the value of 0.0025. To the starting functions we gave the constant value provided by Gouffé's expressions [3] for the bottom of the same enclosure.

For each iteration the calculation time was of about 1–2 and 4 min respectively for $L' = 2-4$ and 8. The iterations number was never greater than six.

In Figs. 2 and 3 we plotted the obtained values for two typical cases, $\epsilon = 0.25-L' = 2$ and $\epsilon = 0.75-L' = 4$. We see

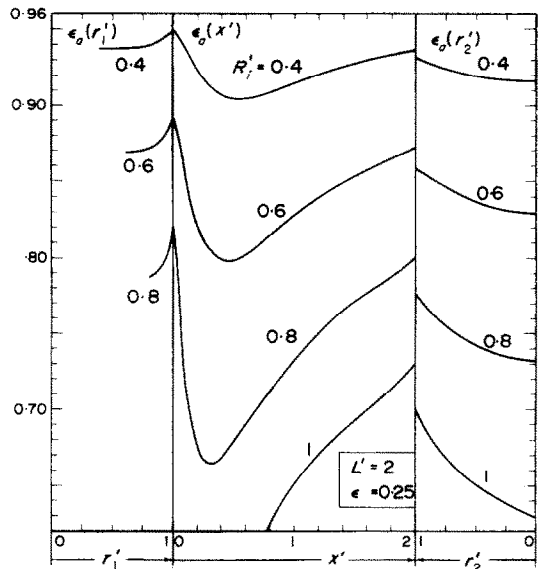


FIG. 2. Apparent thermal emittance in a cylindrical cavity with $\epsilon = 0.25$ and $L' = 2$.

that on the bottom the apparent emittance increases and becomes more uniform as R'_i decreases, that is as the diaphragm aperture becomes smaller. This result is of great interest in applications. On the cylindrical surface the apparent emittance has a minimum which decreases and shifts toward left as R'_i increases. At the corners while for $x' = L'$ there is a values discontinuity, for $x' = 0$ there is only a slope discontinuity. The reason, we think, is that the view factors F_{dA-A_e} , with A_e overall enclosure surface, have different values if dA is at the corner $x' = L'$ on the cylindrical surface or on the bottom, while at the corner $x' = 0$ they are both 1 because in both cases dA does not see the opening.

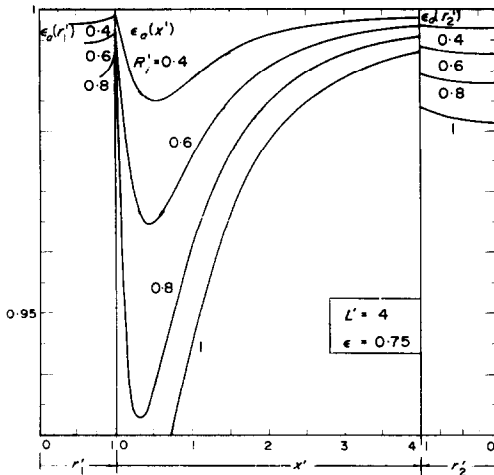


FIG. 3. Apparent thermal emittance in a cylindrical cavity with $\varepsilon = 0.75$ and $L' = 4$.

In Table 1 we have listed the apparent emittance values obtained, for the bottom, at the center and at the corner and for comparison we reported also values obtained by other authors for the same enclosure. A very good agreement is seen among Sparrow's, Peavy's and our results for enclosure without diaphragm. We can also see that the simple Gouffé's method gives good results for $L = 2$. Quinn's method gives good values for $\varepsilon = 0.75$ because he takes into account two reflections only.

REFERENCES

1. E. M. SPARROW, L. U. ALBERS and E. R. G. ECKERT, Thermal radiation characteristics of cylindrical enclosures, *J. Heat Transfer* **84**, 73-81 (1962).
2. B. A. PEAVY, A note on the numerical evaluation of thermal radiation characteristics of diffuse cylindrical and conical cavities, *J. Res. Nat. Bur. Standards* **70C**, 139-147 (1966).
3. A. GOUFFÉ, Corrections d'ouverture des corps noirs artificiels compte tenu des diffusion multiple internes, *Rev. Opt.* **24**, 1-10 (1945).

Table 1. A comparison of apparent emittance values at the bottom

Cavities			$\varepsilon_a(r'_2)$							
L'	ε	R'_1	Gouffé [3] $0 \leq \tau_2 \leq 1$	Quinn [4] $0 \leq \tau_2 \leq 1$	This study		Sparrow [1]		Peavy [2]	
					$r'_2 = 0$	$r'_2 = 1$	$r'_2 = 0$	$r'_2 = 1$	$r'_2 = 0$	$r'_2 = 1$
2	0.25	0.4	0.9177	—	0.9158-0.9311	—	—	—	—	—
		0.6	0.8331	—	0.8289-0.8587	—	—	—	—	—
		0.8	0.7398	—	0.7321-0.7763	—	—	—	—	—
		1	0.6497	—	0.6395-0.6953	—	—	—	0.6401-0.6980	—
	0.50	0.4	0.9683	—	0.9679-0.9771	—	—	—	—	—
		0.6	0.9327	—	0.9316-0.9499	—	—	—	—	—
		0.8	0.8895	—	0.8870-0.9155	—	—	—	—	—
		1	0.8428	—	0.8389-0.8767	—	0.8394-0.8776	—	0.8396-0.8778	—
	0.75	0.4	0.9883	—	0.9882-0.9922	—	—	—	—	—
		0.6	0.9749	—	0.9745-0.9825	—	—	—	—	—
		0.8	0.9581	—	0.9577-0.9699	—	—	—	—	—
		1	0.9394	—	0.9388-0.9552	—	0.9389-0.9553	—	—	—
4	0.25	0.4	0.9586	0.9881	0.9675-0.9724	—	—	—	—	—
		0.6	0.9120	0.9732	0.9312-0.9394	—	—	—	—	—
		0.8	0.8550	0.9524	0.8878-0.9006	—	—	—	—	—
		1	0.7929	0.9245	0.8444-0.8618	—	—	—	0.8442-0.8612	—
	0.50	0.4	0.9872	0.9930	0.9902-0.9919	—	—	—	—	—
		0.6	0.9720	0.9844	0.9786-0.9820	—	—	—	—	—
		0.8	0.9518	0.9722	0.9635-0.9689	—	—	—	—	—
		1	0.9277	0.9560	0.9460-0.9537	—	0.9460-0.9540	—	0.9460-0.9534	—
	0.75	0.4	0.9962	0.9970	0.9968-0.9978	—	—	—	—	—
		0.6	0.9916	0.9932	0.9929-0.9943	—	—	—	—	—
		0.8	0.9854	0.9880	0.9878-0.9898	—	—	—	—	—
		1	0.9776	0.9812	0.9815-0.9839	—	0.9815-0.9842	—	—	—
8	0.25	0.4	0.9787	0.9976	0.9901-0.9920	—	—	—	—	—
		0.6	0.9536	0.9945	0.9814-0.9830	—	—	—	—	—
		0.8	0.9210	0.9902	0.9688-0.9709	—	—	—	—	—
		1	0.8830	0.9843	0.9645-0.9671	—	—	—	—	—
	0.50	0.4	0.9944	0.9985	0.9976-0.9981	—	—	—	—	—
		0.6	0.9874	0.9966	0.9951-0.9957	—	—	—	—	—
		0.8	0.9780	0.9949	0.9918-0.9925	—	—	—	—	—
		1	0.9664	0.9920	0.9886-0.9894	—	0.9880-0.9887	—	—	—
	0.75	0.4	0.9986	0.9993	0.9992-0.9999	—	—	—	—	—
		0.6	0.9970	0.9984	0.9983-0.9990	—	—	—	—	—
		0.8	0.9946	0.9972	0.9971-0.9978	—	—	—	—	—
		1	0.9916	0.9957	0.9956-0.9958	—	0.9956-0.9961	—	—	—

4. T. J. QUINN, The calculation of the emissivity of cylindrical cavities giving near black-body radiation, *Br. J. Appl. Phys.* **18**, 1105–1113 (1967).
5. E. M. SPARROW and R. D. CESS, *Radiation Heat Transfer*, p. 133. Brooks/Cole, Belmont, California (1966).
6. T. J. LOVE, *Radiative Heat Transfer*, pp. 92–94. Charles E. Merrill, Columbus, Ohio (1968).
7. K. S. KUNZ, *Numerical Analysis*, pp. 343–344. McGraw-Hill, New York (1957).

Int. J. Heat Mass Transfer. Vol. 15, pp. 2674–2679. Pergamon Press 1972. Printed in Great Britain

ON THE HEAT TRANSFER ASPECTS OF VAPOR DEPOSITION *IN VACUO*

J. SZEKELY and J. J. POVEROMO

Department of Chemical Engineering and Center for Process Metallurgy,
State University of New York at Buffalo, Buffalo, New York 14214, U.S.A.

NOMENCLATURE

E ,	rate of vaporization;
F ,	view factor;
H_t ,	latent heat of sublimation;
L ,	thickness of the backing plate;
M ,	molecular weight of the metal;
P ,	vapor pressure;
R ,	gas constant;
T ,	temperature;
t ,	time;
V ,	residual pressure;
$Y(t)$,	position of the condensing surface at time t ;
y ,	distance coordinate.

Greek symbols

δ ,	vaporization coefficient;
ϵ ,	emissivity;
κ ,	thermal diffusivity;
ρ ,	density;
σ ,	Stefan-Boltzmann constant.

Subscripts

s ,	source surface;
c ,	condensing surface;
net,	net rate;
b ,	backing plate;
d ,	deposit;
m ,	melting point.

1. INTRODUCTION

THE DEPOSITION of metals vapors onto surfaces *in vacuo* plays an important role both in materials finishing operations and in separation processes. A common feature of

these operations is that there exists a molten metal pool, which acts as the source of the vapor, in the proximity of an initially cold surface onto which the vapor is deposited. Depending on the actual application, the sink or receptor surface may be moving or may be stationary.

By far the greatest practical application of vapor deposition techniques is the formation of coatings, and for this reason most of the attention has been focused on the molecular aspects of the problem and on the factors that influence the physical nature of the deposit [1–4].

Vapor deposition as a separation technique is used in the dezincing of lead and the thermodynamic and molecular aspects of this problem were treated by Davey [5–7].

In contrast to the extensive work done on the molecular and thermodynamic aspects of vapor deposition, the heat transfer aspects of this problem received very little attention up to the present. The motivation for the study of the thermal phenomena, associated with vapor deposition may be twofold: the heat generated by the formation of the solid deposit will raise the temperature of both the deposit and that of the receptor. These changes in temperature may affect the nature of the deposit and the nature of the bonding between the deposit and the substrate-factors that may be significant in coating operations.

Furthermore, the generation of heat may raise the temperature of the outer surface of the deposit to levels, where “back vaporization” may become significant or where ablation melting may occur. Under these conditions thermal effects will limit the net rate of deposition that may be achieved. This particular group of problems is most likely to be important in separation processes. In the following we shall present a formulation of the thermal problem together with the numerical solution of the